Expert Systems With Applications 55 (2016) 268–273

Contents lists available at ScienceDirect

Expert Systems With Applications

journal homepage: www.elsevier.com/locate/eswa

A variational mode decompoisition approach for analysis and forecasting of economic and financial time series

Salim Lahmiri*

ESCA School of Management, 7 Abou Youssef El Kindy Street, BD Moulay Youssef, Casablanca, Morocco

ARTICLE INFO

Keywords:
Empirical mode decomposition
Variational mode decomposition
Time series
Regression
Neural network
Forecasting

ABSTRACT

The empirical mode decomposition (EMD) has been successfully applied to adaptively decompose economic and financial time series for forecasting purpose. Recently, the variational mode decomposition (VMD) has been proposed as an alternative to EMD to easily separate tones of similar frequencies in data where the EMD fails. The purpose of this study is to present a new time series forecasting model which integrates VMD and general regression neural network (GRNN). The performance of the proposed model is evaluated by comparing the forecasting results of VMD-GRNN with three competing prediction models; namely the EMD-GRNN model, feedforward neural networks (FFNN), and autoregressive moving average (ARMA) process on West Texas Intermediate (WTI), Canadian/US exchange rate (CANUS), US industrial production (IP) and the Chicago Board Options Exchange NASDAQ 100 Volatility Index (VIX) time series are used for experimentations. Based on mean absolute error (MAE), mean absolute percentage error (MAPE), and the root mean of squared errors (RMSE), the analysis results from forecasting demonstrate the superiority of the VMD-based method over the three competing prediction approaches. The practical analysis results suggest that VMD is an effective and promising technique for analysis and prediction of economic and financial time series.

1. Introduction

Huang et al. (1998) introduced an adaptive technique called empirical mode decomposition (EMD) to represent nonlinear and nonstationary signals as sums of components with amplitude and frequency modulated parameters. In particular, it is a multiresolution technique to perform the joint space-spatial frequency decomposition of a signal empirically by successive removal of elemental signals, the intrinsic mode functions or IMF, which represent the oscillatory modes of the original signal going from high- to low-frequency ranges. The obtained IMFs can then serve to represent the signal. The intrinsic mode function is complete, adaptive and almost orthogonal. The main advantage of using the EMD technique is that the input signal is analyzed without need to convolve it with a basis function as done for Fourier and wavelet transforms. In addition, the method is data driven and, thus, self-adaptive. These features make EMD suitable for nonlinear and non-stationary data analysis. Because of its attractive features, it was applied in diverse scientific areas of signal processing; including mechanical engineering (Ricci & Pennacchi, 2011), signal de-noising (Li, Wang, Tao, Wang, & Du, 2011, Lahmiri and Boukadoum, 2014a, 2015a), speaker identification (Wu et al, 2011), biomedical image analysis (Ai, Wang, & Yao, 2011, Lahmiri & Boukadoum, 2014b, 2015b), DNA sequence analysis (Zhang et al, 2012), and machinery fault diagnosis (Cheng, Yang, & Yang, 2012).

The EMD has also received a large attention in analysis of economic and financial data for forecasting purpose. For instance, it was employed in modeling and predicting crude oil price (Zhang, Lai, & Wang, 2008; Zhang, Yu, Wang, & Lai, 2009), stock market (Cheng et al, 2014), electricity price (An, Zhao, Wang, Shang, & Zhao, 2013, Lisi & Nan, 2014), and foreign exchange rate (Lin, Chiu, & Lin, 2012, Premanode & Toumazou, 2013).

More recently, a new multiresolution called variational mode decomposition (VMD) was introduced by Dragomiretskiy and Zosso (2014) as an alternative to the EMD algorithm to overcome its limits. For instance, drawbacks of the EMD include lack of exact mathematical model, interpolation choice, and sensitivity to both noise and sampling (Dragomiretskiy & Zosso, 2014). The VMD is an entirely non-recursive variational model where the modes are extracted concurrently (Dragomiretskiy & Zosso, 2014). In particular, the VMD model searches for a number of modes and their respective center frequencies, such that the band-limited modes reproduce the input signal exactly or in least-squares sense (Dragomiretskiy & Zosso, 2014). In sum, the VMD has the

* Corresponding author. Tel.: +212 522 20 91 20.
E-mail address: slahmiri@esca.ma

http://dx.doi.org/10.1016/j.eswa.2016.02.025
0957-4174/

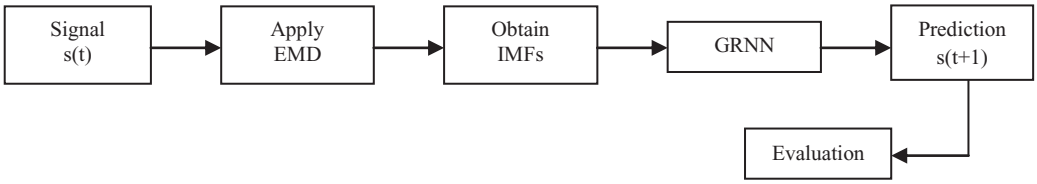

Fig. 1. EMD-based system.

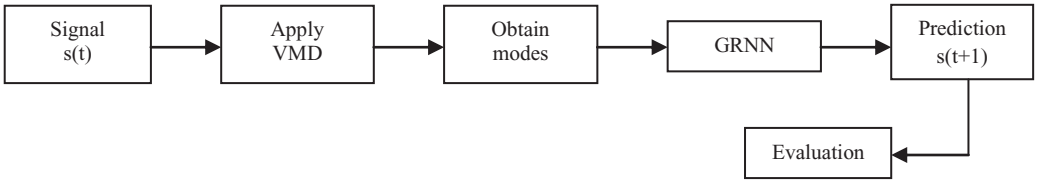

Fig. 2. VMD-based system.

ability to separate tones of similar frequencies contrary to the EMD (Dragomiretskiy & Zosso, 2014). Using simulated harmonic functions, Dragomiretskiy and Zosso (2014) found that the VMD as a denoising approach outperforms the EMD. The VMD was found to be effective in biomedical signal denoising (Lahmiri & Boukadoum, 2014c, 2015c) and also was applied in analysis of international stock markets (Lahmiri, 2015d). However, there is a need to explore the effectiveness of the VMD against the EMD in modeling and forecasting economic and financial data. Indeed, modeling and forecasting economic and financial data is crucial for government to set economic policy and for companies to manage portfolios and control risk.

The objective of this study is to explore the usefulness of the VMD in extracting economic and financial time series features (components) for prediction purpose. In particular, we compare the performance of the EMD and VMD based approach in terms of forecasting accuracy of four economic and financial data: West Texas Intermediate (WTI) (crude oil), Canadian/US exchange rate, US industrial production (IP), and the Chicago Board Options Exchange NASDAQ 100 Volatility Index (VIX).

Finally, the performance of each approach will be assessed by virtue of statistical performance measures they are the mean absolute error (MAE), mean absolute percentage error (MAPE), and the root mean of squared errors (RMSE). The general regression neural network (GRNN) (Specht, 1991) will be used for training and testing the EMD and VMD extracted patterns. The GRNN is chosen since it provides fast learning and convergences to the optimal regression surface as the number of samples becomes very large (Polat & Yildirim, 2008). In this work, a feedforward neural network (FFNN) (Haykin, 2008) trained with past observations and the well-known autoregressive moving average (ARMA) process will also be considered as baseline models for comparison purpose.

The remaining of the paper is organized as follows. In Section 2 briefly introduces the empirical mode decomposition, the variational mode decomposition, and the general regression neural network. The obtained simulation results are provided in Section 3 while Section 4 concludes.

2. Methods

Two main prediction systems are designed, evaluated, and compared. In the first system, the EMD is applied to the original data (signal) to obtain its intrinsic mode functions (IMFs). Then, they will be fed to the GRNN for forecasting purpose. Similarly, in the second system the VMD is applied to the original data (signal) to obtain its variational modes. Then, the latter will be fed to the GRNN for forecasting purpose. The two forecasting systems are described in Figs. 1 and 2 respectively. The EMD, VMD, GRNN, and statistical performance measures are described next.

2.1. Empirical mode decomposition

The key feature of the EMD is to decompose a signal into a sum of functions such that each of them has the same numbers of zero crossings and extrema, and is symmetric with respect to its local mean (Huang et al., 1998). These are the so called Intrinsic Mode Functions (IMFs). The IMFs are found at each scale going from fine to coarse by an iterative procedure called sifting algorithm. For a signal s(t), the EMD decomposition is performed as follows (Liu, Xu, & Li, 2007):

(a) Find all the local maxima, $M_i, i = 1, 2, \ldots,$and minima, $m_k, k = 1, 2, \ldots,$in $s(t)$.

(b) Compute by interpolation -for instance a cubic Spline- the upper and lower envelopes of the signal: $M(t) = f_M(M_i, t)$ and$m(t) = f_m(m_i, t)$.

(c) Compute the envelope mean $e(t)$ as the average of the upper and lower envelopes: $e(t) = (M(t) + m(t))/2$.

(d) Compute the details as:$d(t) = s(t) - e(t)$.

(e) Check the properties of $d(t)$:(e.1) If $d(t)$ meets the conditions on number of extrema and symmetry stated previously, compute the ith IMF as $IMF(t) = d(t)$ and replace s(t) with the residual $r(t) = s(t) - IMF(t)$.

(e.2) If $d(t)$ is not an IMF, then replace $s(t)$ with the detail: $s(t) = d(t)$.

(f) Iterate steps (a) to (e) until the residual $r(t)$ satisfies a given stopping criterion.

In the end, $s(t)$ is expressed as follows:

$$s(t) = \sum_{j=1}^{N} IMF_j(t) + r_N(t) \tag{1}$$

where N is the number of IMF which are nearly orthogonal to each other and all have nearly zero means; and $r_n(t)$ is the final residue which is the low frequency trend of the signal $s(t)$. Usually, the standard deviation (SD) computed from two consecutive sifting results is used as criterion to stop the sifting process by limiting the SD size (Huang et al., 1998; Chen et al., 2009) as:

$$SD(k) = \frac{\sum_{t=0}^{T} |d_{k-1}(t) - d_k(t)|^2}{\sum_{t=0}^{T} d_{k-1}^2(t)} < \varepsilon \tag{2}$$

where k is the index of the kth difference between the signal $s(t)$ and the envelope mean $e(t)$. The term ε is a pre-determined stopping value. For instance, its value is set to 0.001.

2.2. Variational mode decomposition

The purpose of the VMD is to decompose an input signal into k discrete number of sub-signals (modes), where each mode has limited bandwidth in spectral domain (Dragomiretskiy & Zosso, 2014). Thus, each mode k is required to be mostly compact around a center pulsation ω_k determined along with the decomposition (Dragomiretskiy & Zosso, 2014). The VMD algorithm to assess the bandwidth of a one dimension signal is as follows (Dragomiretskiy & Zosso, 2014): (1) for each mode u_k, compute the associated analytic signal by means of the Hilbert transform to obtain a unilateral frequency spectrum, (2) for each mode, shift the mode's frequency spectrum to baseband by mixing with an exponential tuned to the respective estimated center frequency, (3) estimate the bandwidth through Gaussian smoothness of the demodulated signal; for example, the squared L2-norm of the gradient. Then, the constrained variational problem is given by Dragomiretskiy & Zosso, (2014):

$$\min_{u_k,\,\omega_k} = \left\{ \sum_k \left\| \partial_t \left[\left(\delta(t) + \frac{j}{\pi t} \right) * u_k(t) \right] e^{-j\omega_k t} \right\|_2 \right\} \tag{3}$$

Subject to,

$$\sum_k u_k = f \tag{4}$$

where f is the signal, u is its mode, ω is the frequency, δ is the Dirac distribution, t is time script, k is number of modes, and $*$ denotes convolution. The mode u with high-order k represents low frequency components.

2.3. General regression neural network

The GRNN (Specht, 1991) is a parallel and memory-based system that estimates the regression surface of a continuous variable. It is a one pass learning algorithm; thus provides fast learning and convergences to the optimal regression surface when sample size is large (Specht, 1991). Assume that the system input is the vector X, and the desired estimate of the system output is the vector Y. Suppose that the joint continuous probability density function of X and Y is represented by an unknown function $f(x,y)$. Then, the regression of y on x is represented by:

$$E[y|X=x] = \frac{\int_{-\infty}^{+\infty} y\, f(x,y)dy}{\int_{-\infty}^{+\infty} f(x,y)dy} \tag{5}$$

The unknown joint continuous probability density function $f(x,y)$ is estimated as follows:

$$\hat{f}(X,y) = \frac{1}{2\pi^{(p+1)/2}\sigma^{(p+1)}} \times n^{-1} \times \left\{ \sum_{i=1}^{n} \exp\left[-\frac{(X-X_i)^T(X-X_i)}{2\sigma^2} \right] \times \exp\left[-\frac{(Y-Y_i)^2}{2\sigma^2} \right] \right\} \tag{6}$$

where $\sigma < 1$ is the width of the Gaussian kernel, p is the dimension of X, and n is the sample size. When $\hat{f}(X,y)$ is substituted in$E[y|X=x]$, then the output function $Y(X)$ is given by:

$$Y(X) = \frac{\sum_{i=1}^{n} Y_i \exp\left[-\frac{D_i^2}{2\sigma^2} \right]}{\sum_{i=1}^{n} \exp\left[-\frac{D_i^2}{2\sigma^2} \right]} \tag{7}$$

where $D_i^2$is expressed as follows:

$$D_i^2 = (X-X_i)^T(X-X_i) \tag{8}$$

The GRNN consists of four layers, including the input layer, pattern layer, summation layer, and output layer. The input layer is fully connected to the pattern layer, where each unit represents a training pattern. For instance, each neuron in the input layer represents a given variational function when VMD is employed (VMD-GRNN model) or an intrinsic mode function when EMD (EMD-GRNN model) is employed instead. The pattern layer consists of pattern units which represent all the training samples. Outputs of the pattern layer are passed on to the summation layer where a dot product between a weight vector composed of the signals from the pattern units is performed. Finally, the output layer yields the predicted value corresponding to an unknown input vector; for instance the predicted value of the time series. Recall that for comparison purpose, a feedforward neural network (FFNN) (Haykin, 2008) trained with the five past observations and the well-known autoregressive moving average (ARMA) process will also be employed to assess the effectiveness of the presented VMD-GRNN model.

2.4. Performance measures

The forecasting performance is evaluated using the following performance measures: the mean absolute error (MAE), mean absolute percentage error (MAPE), and the root mean of squared errors (RMSE). They measure the deviation between actual and predicted values. The smaller values of MAE, MAPE, and RMSE, the closer are the predicted time series values to that of the actual value. Thus, they can be used to evaluate the prediction error. The definitions of these criteria are given as follows:

$$MAE = \frac{\sum_{i=1}^{n} |A_i - P_i|}{n} \tag{9}$$

$$MAPE = \frac{1}{n} \sum_{i=1}^{n} \left| \frac{A_i - P_i}{A_i} \right| \times 100\% \tag{10}$$

$$RMSE = \sqrt{\frac{\sum_{i=1}^{n} (A_i - P_i)^2}{n}} \tag{11}$$

where A and P represent, respectively the actual and predicted value; and n is total number of out-of-sample data points.

3. Results

Daily data of the West Texas Intermediate (WTI), Canadian/US exchange rate (CANUS), and the Chicago Board Options Exchange NASDAQ 100 Volatility Index (VIX), monthly data of the US industrial production (IP) from January 2nd 2008 to December 16th 2013 were used to conduct experiments. They were obtained from the Federal Bank of Saint Louis, USA. The first 80% of the samples are used for training the GRNN and the remaining 20% are used for testing. Figs. 3–6 exhibit WTI, CANUS, IP, and VIX time series, where x-axis is observation number and y-axis is observed values. Examples of IMFs and modes obtained respectively by EMD and VMD for IP time series are illustrated in Figs. 7 and 8.

Since the VMD requires a predetermined number of decomposition k, the latter is varied depending on the number of IMFs obtained by EMD. For instance, if the number of IMFs is d, then the parameter k used to determine the number of decomposition to obtain by EMD is d–3, d–2, d–1, d, d+1, d+2, and d+3. The simulation results for WTI, Canadian/US exchange rate, industrial production, and NASDAQ 100 Volatility Index are respectively shown in Tables 1–4. According to MAE, MAPE, and RMSE values shown in Table 1 the forecasting approach based on VMD outperformed the EMD-based approach in predicting the future crude oil prices. This is true for all values of k. Similarly, the forecasting approach based on VMD outperformed the EMD-based approach in predicting the Canadian/US exchange rate for all values of k according to

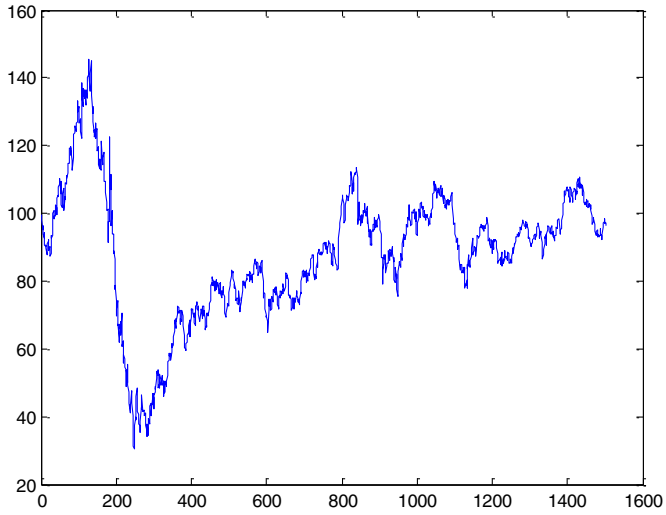

Fig. 3. WTI time series.

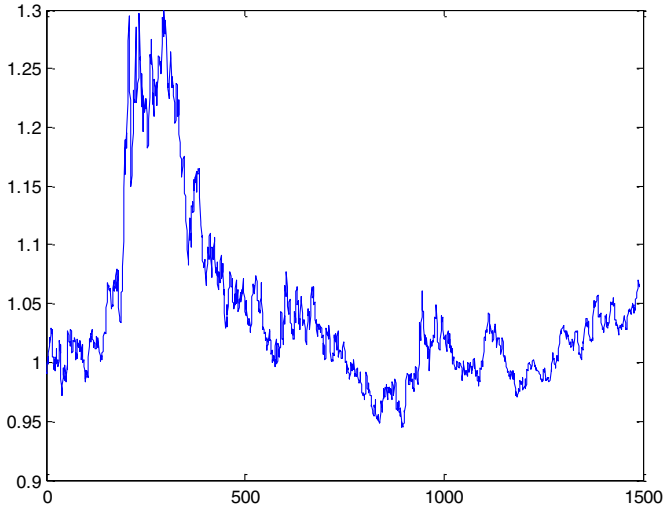

Fig. 4. Canadian/US exchange rate time series.

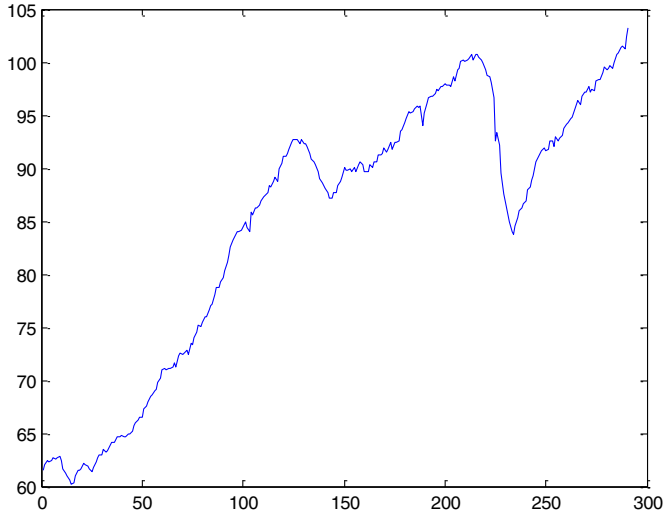

Fig. 5. IP time series.

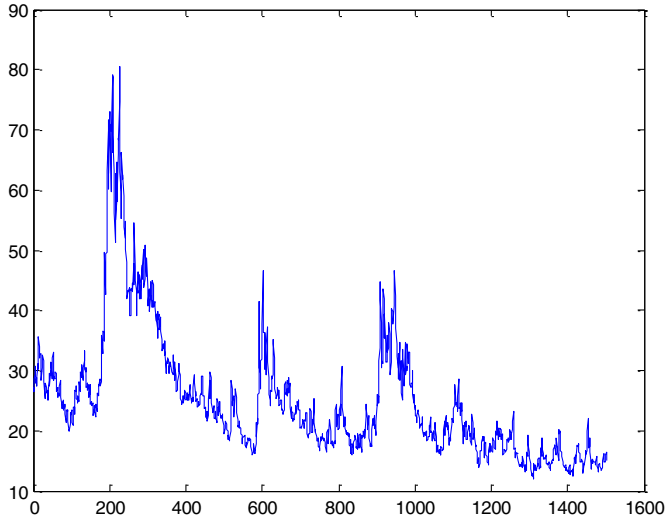

Fig. 6. VIX time series.

Table 1
Performance for the WTI time series.

	MAE	MAPE	RMSE
EMD	11.4755	12.7085	25.2435
VMD ($K=6$)	1.6032	1.6183	2.1201
VMD ($K=7$)	1.5997	1.6143	2.1210
VMD ($K=8$)	1.5795	1.5933	2.1094
VMD ($K=9$)	1.7255	1.7439	2.2550
VMD ($K=10$)	1.7232	1.7427	2.2475
VMD ($K=11$)	1.7826	1.8105	2.3055
VMD ($K=12$)	1.8786	1.9291	2.3961
FFNN	61.9352	64.3726	62.2902
ARMA	96.9726	97.1308	116.7510

MAE, MAPE, and RMSE values shown in Table 2. For the US industrial production, EMD-based approach performs better than VMD with $k=7$ in terms of MAE and MAPE As shown in Table 3. It also performs better than VMD in terms of RMSE with $k=4$, 5, 6, 7. In sum, the lowest values of MAE, MAPE, and RMSE are with $k=8$ when VMD approach is adopted; as a result, it outperforms the EMD-based approach for predicting US industrial production. Finally, Table 4 shows that the forecasting approach based on VMD outperformed the EMD-based approach in predicting the NASDAQ 100 Volatility Index as indicated by MAE, MAPE, and RMSE values for all values of k. Finally, Tables 1–4 demonstrate that the presented VMD-GRNN prediction system outperformed the FFNN trained with historical observations and also the classical ARMA process in terms of all performance measures in predicting West Texas Intermediate, Canadian/US exchange rate, US industrial production, and the Chicago Board Options Exchange NASDAQ 100 Volatility Index.

In summary, the experimental results fully illustrate the advantage of the VMD-based model for forecasting economic and financial data. Indeed, the advantage of EMD-based filtering is apparent based on four data sets and statistical performance measures used in this study.

The possible reasons that the EMD decomposition impacts the prediction performance could be two-fold. On one hand, the VMD model searches for a number of modes and their respective center frequencies, such that the band-limited modes reproduce the input signal exactly or in least-squares sense. In particular, it has the ability to separate tones of similar frequencies contrary to the EMD. On the other hand, VMD is more robust to noisy data such as the WTI, Canadian/US exchange rate, industrial production, and

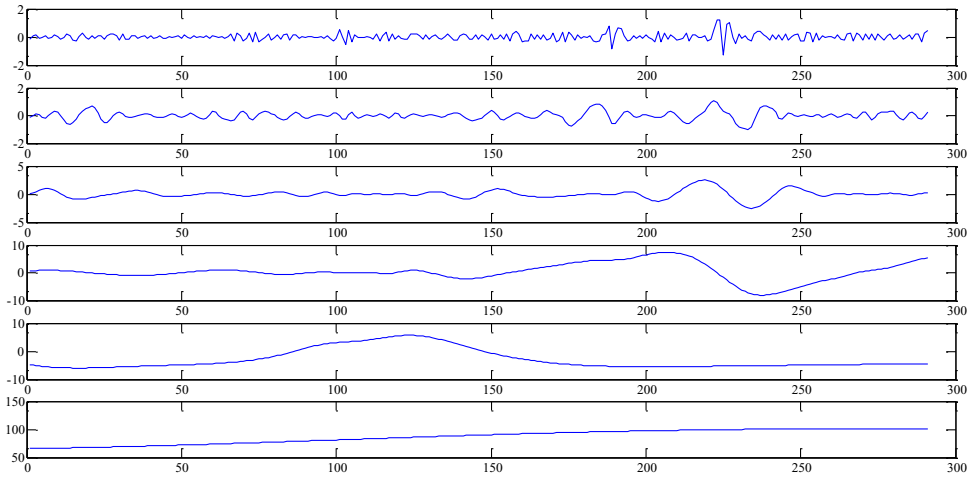

Fig. 7. EMD decomposition results for IP time series. From top to bottom: first IMF to residue.

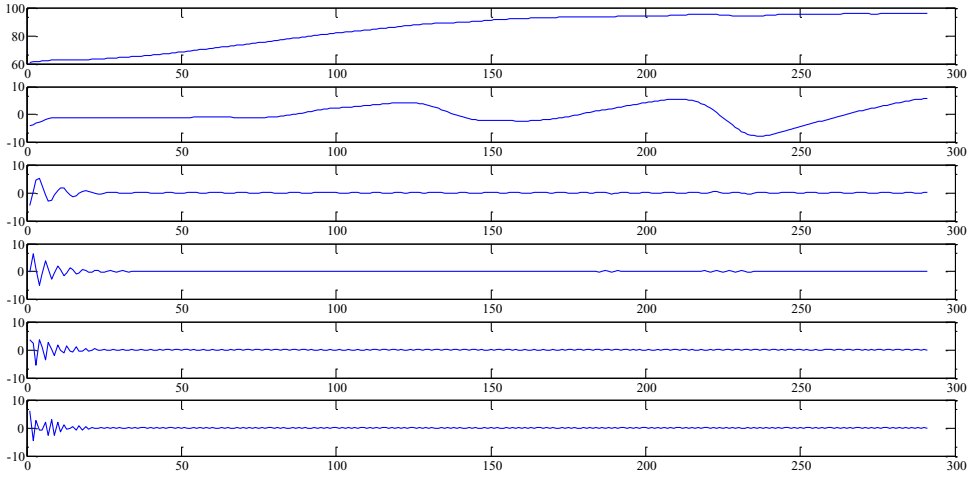

Fig. 8. VMD decomposition results for IP time series. From top to bottom: first mode to sixth one.

Table 2
Performance for CANUS time series.

	MAE	MAPE	RMSE
EMD	0.0294	2.9286	0.0358
VMD ($K=6$)	0.0289	2.8773	0.0352
VMD ($K=7$)	0.0289	2.8774	0.0352
VMD ($K=8$)	0.0289	2.8781	0.0352
VMD ($K=9$)	0.0289	2.8811	0.0353
VMD ($K=10$)	0.0289	2.8813	0.0353
VMD ($K=11$)	0.0291	2.9016	0.0355
VMD ($K=12$)	0.0292	2.9030	0.0355
FFNN	0.2524	24.7592	0.2535
ARMA	0.8979	8.7801	1.1152

Table 3
Performance for IP time series.

	MAE	MAPE	RMSE
EMD	1.3583	1.4646	1.6289
VMD (K=6)	1.0881	1.1791	1.4771
VMD (K=7)	1.2513	1.3546	1.7439
VMD (K=8)	1.2709	1.3755	1.7670
VMD (K=9)	1.2832	1.3884	1.7834
VMD (K=10)	1.4067	1.5203	1.8818
VMD (K=11)	0.9144	0.9627	1.0959
VMD (K=12)	0.9241	0.9733	1.1070
FFNN	14.1580	14.5833	16.2013
ARMA	53.4600	57.7455	66.3919

Table 4
Performance for VIX time series.

	MAE	MAPE	RMSE
EMD	3.8437	25.5625	4.3238
VMD (K=6)	1.6735	11.3780	1.9330
VMD (K=7)	1.6727	11.3716	1.9322
VMD (K=8)	1.6919	11.4742	1.9407
VMD (K=9)	1.6939	11.4883	1.9428
VMD (K=10)	1.6922	11.4732	1.9422
VMD (K=11)	1.6916	11.4667	1.9419
VMD (K=12)	1.6932	11.4766	1.9434
FFNN	37.2400	25.1600	38.3200
ARMA	9.3023	62.3786	10.0399

NASDAQ 100 Volatility Index. Indeed, as each mode is updated by Wiener filtering in Fourier domain during the optimization process, the updated mode is less affected by noisy disturbances. In this regard, the VMD can appropriately capture signal short and long variations better than the EMD.

4. Conclusion

The purpose of the paper was to present a predictive system for economic and financial data by using VMD; which is a new adaptive multiresolution technique; in conjunction with GRNN model. In this regard, we compared the forecasting accuracy of four

economic and financial data sets using VMD-based GRNN model against EMD-based approach, feedforwar neural network and ARMA process. Experiments with different statistical criteria (MAE, MAPE, RMSE), clearly demonstrate that VMD-based GRNN model significantly achieved the lowest forecasting error for all data sets. This indicates that the VMD-based general regression neural network forecasting paradigm can be used as a very promising methodology for world economic and financial prediction. In sum, this work is an important step in time series modeling and forecasting as it highlights the use of VMD in an intelligent expert system framework for predicting economic and financial data.

The main advantages of adopting the VMD-GRNN approach are twofold. First, as a new adaptive multiresolution technique, the VMD is more robust to analyze noisy signals such as economic and financial data than EMD. Second, the GRNN is a one pass learning algorithm; thus it provides fast learning and convergence when the sample size is large. As a result, the VMD-GRNN approach is suitable to analyze noisy data and fast processing and convergence when dealing with large dataset. Indeed, the proposed predictive system is not cumbersome, simple to implement, and easy to understand. All these make it very attractive to users.

However, the VMD algorithm requires predetermining the number of variational modes to be extracted contrary to the EMD. It is not easy to set a rule to determine an appropriate number of variational modes. For simplicity, we may suggest to fix it equal to the number of extracted intrinsic mode functions by EMD. However, a formal methodology should be developed in this regard in future works.

Indeed, with regards to the future research directions, we can extend this study by applying the presented model to forecasting intraday stock prices, asset volatility prediction, and economic and financial time series classification. For instance, the validity of the VMD-GRNN can be tested on prediction of time series future upward and downward movements. Finally, a comparative study of accuracy of the VMD combined with other data mining models such as support vector machines and radial basis function neural networks could be considered for future works to examine the effectiveness of the VMD-GRNN model.

References

Ai, L., Wang, J., & Yao, R. (2011). Classification of parkinsonian and essential tremor using empirical mode decomposition and support vector machine. *Digital Signal Processing, 21*, 543–550.

An, N., Zhao, W., Wang, J., Shang, D., & Zhao, E. (2013). Using multi-output feedforward neural network with empirical mode decomposition based signal filtering for electricity demand forecasting. *Energy, 49*, 279–288.

Cheng, C.-H., & Wei, L.-Y. (2014). A novel time-series model based on empirical mode decomposition for forecasting TAIEX. *Economic Modeling, 36*, 136–141.

Cheng, J., Yang, Y., & Yang, Y. (2012). A rotating machinery fault diagnosis method based on local mean decomposition. *Digital Signal Processing, 22*, 356–366.

Dragomiretskiy, K., & Zosso, D. (2014). Variational mode decomposition. *IEEE Transactions on Signal Processing, 62*, 531–544.

Haykin, S. O. (2008). *Neural networks and learning machines* (3rd). Upper Saddle River, New Jersey: Prentice Hall.

Huang, N. E., Shen, Z., Long, S. R., Wu, M. C., Shih, H. H., Zheng, Q., Yen, N.-C., Tung, C. C., & Liu, H. H. (1998). The empirical mode decomposition and the Hilbert spectrum for non-linear and non-stationary time series analysis,". *Proc. R. Soc., Lond., A, 454*, 903–995.

Lahmiri, S. (2014a). A comparative study of ecg signal denoising by wavelet thresholding in empirical and variational mode decomposition domains. *IET Healthcare Technol. Lett., 1*, 104–109.

Lahmiri, S., & Boukadoum, M. (2015a). A weighted bio-signal denoising approach using empirical mode decomposition. *Biomed. Eng. Lett., 5*, 131–139.

Lahmiri, S., & Boukadoum, M. (2014b). Automated detection of circinate exudates in retina digital images using empirical mode decomposition and the entropy and uniformity of intrinsic mode functions. *Biomedizinische Technik/Biomedical Engineering, 59*, 357–366.

Lahmiri, S., & Boukadoum, M. (2015b). Pathology grading in retina digital images using student-adjusted empirical mode decomposition and power law statistics. *IEEE LASCAS*, 1–4.

Lahmiri, S., & Boukadoum, M. (2014c). Biomedical image denoising using variational mode decomposition. *IEEE BIOCAS*, 340–343.

Lahmiri, S., & Boukadoum, M. (2015c). Physiological signal denoising with variational mode decomposition and weighted reconstruction after DWT thresholding. *IEEE ISCAS*, 806–809.

Lahmiri, S. (2015d). Long memory in international financial markets trends and short movements during 2008 financial crisis based on variational mode decomposition and detrended fluctuation analysis. *Physica A, 437*, 130–138.

Li, C., Wang, X., Tao, Z., Wang, Q., & Du, S. (2011). Extraction of time varying information from noisy signals: an approach based on the empirical mode decomposition. *Mechanical Systems and Signal Processing, 25*, 812–820.

Lin, C.-S., Chiu, S.-H., & Lin, T.-Y. (2012). Empirical mode decomposition–based least squares support vector regression for foreign exchange rate forecasting. *Economic Modeling, 29*, 2583–2590.

Lisi, F., & Nan, F. (2014). Component estimation for electricity prices: procedures and comparisons. *Energy Economics, 44*, 143–159.

Liu, W., Xu, W., & Li, L. (2007). Medical image retrieval based on bidimensional empirical mode decomposition. *IEEE International Conference on Bioinformatics and Bioengineering*, 641–646.

Polat, O., & Yildirim, T. (2008). Hand geometry identification without feature extraction by general regression neural network. *Expert Systems with Applications, 34*, 845–849.

Premanode, B., & Toumazou, C. (2013). Improving prediction of exchange rates using Differential EMD. *Expert Systems with Applications, 40*, 377–384.

Ricci, R. R., & Pennacchi, P. (2011). Diagnostics of gear faults based on EMD and automatic selection of intrinsic mode functions. *Mechanical Systems and Signal Processing, 25*, 821–838.

Specht, D. F. (1991). A general regression neural network. *IEEE Transactions on Neural Networks, 6*, 568–576.

Wu, J.-D., & Tsai, Y.-J. (2011). Speaker identification system using empirical mode decomposition and an artificial neural network. *Expert Systems with Applications, 38*, 6112–6117.

Zhang, W.-F., & Yan, H. (2012). Exon prediction using empirical mode decomposition and Fourier transform of structural profiles of DNA sequences. *Pattern Recognition, 45*, 947–955.

Zhang, X., Lai, K. K., & Wang, S.-Y. (2008). A new approach for crude oil price analysis based on empirical mode decomposition. *Energy Economics, 30*, 905–918.

Zhang, X., Yu, L., Wang, S., & Lai, K. K. (2009). Estimating the impact of extreme events on crude oil price: an EMD-based event analysis method. *Energy Economics, 31*, 768–778.